

Development and Characterization of Mesalamine Nanoparticles for Effective Targeting of Ulcerative Colitis

Rameshwar Rajput¹, Eisha Ganju^{1*}, Bhaskar Kumar Gupta¹

¹School of Pharmacy & Research, People's University, Bhopal 462037, Madhya Pradesh, India

ABSTRACT

Aim: To develop and characterize mesalamine-loaded nanoparticles for enhanced efficacy and targeted delivery in the treatment of ulcerative colitis (UC), addressing the limitations of conventional mesalamine therapies.

Methodology: Mesalamine nanoparticles were formulated using the solvent evaporation technique and optimized for particle size, morphology, drug loading efficiency, and release kinetics. Dynamic light scattering (DLS), scanning electron microscopy (SEM), and Fourier-transform infrared spectroscopy (FTIR) were employed for comprehensive characterization. In vitro drug release studies assessed the sustained release profile, and pharmacokinetic studies evaluated the nanoparticles' localized drug delivery potential to inflamed colonic tissues.

Results: The formulated mesalamine nanoparticles exhibited a mean particle size of 150 ± 20 nm with a narrow size distribution and a high drug loading capacity of $85 \pm 5\%$. DLS and SEM analyses confirmed uniform morphology and particle stability, while FTIR verified successful drug encapsulation. In vitro studies demonstrated a sustained mesalamine release over an extended period, outperforming conventional formulations. Pharmacokinetic studies further revealed enhanced localization and prolonged drug availability in inflamed tissues, indicating improved therapeutic efficacy.

Conclusion: Mesalamine-loaded nanoparticles offer a promising drug delivery system for ulcerative colitis, significantly enhancing bioavailability and targeted delivery. This novel approach could overcome the limitations of traditional therapies, providing more effective management of UC and improving patient outcomes.

Keywords: Mesalamine, Nanoparticles, Ulcerative Colitis, Targeted Drug Delivery, Nanotechnology, Anti-inflammatory

INTRODUCTION

Ulcerative colitis (UC) causes irritation and ulcers (open sores) in your large intestine. It belongs to a group of conditions called inflammatory bowel disease (IBD). It often causes diarrhea with blood, cramping and urgency. Sometimes, these symptoms can wake you up at night to go to the bathroom. The inflammation in ulcerative colitis usually starts in your rectum, which is close to your anus. The inflammation can spread and affect a portion of your entire colon. When the inflammation occurs in your rectum and lower part of your colon, it's called ulcerative proctitis. If the entire large intestine is affected, it's called pancolitis. If only the left side of your colon is affected, it's called limited or distal colitis.¹

The severity of UC depends on the amount of inflammation and the location. Everyone is a little different. You could have severe inflammation in your rectum (small area) or very mild inflammation in your entire colon (large area). Doctors can notice a pattern of flare-ups (active disease), when symptoms are worse. During times of remission, you might have little to no symptoms. The goal of therapy is to remain in remission as long as possible (years). About half of the people diagnosed with ulcerative colitis have mild symptoms. Others experience frequent fevers, bloody diarrhea, nausea and severe abdominal cramps. Ulcerative colitis may also cause issues such as arthritis, inflammation of the eye, liver disease and osteoporosis. It isn't known why these problems occur outside of your colon. Scientists

Corresponding Author:

Dr. Eisha Ganju, Professor, School of Pharmacy & Research, People's University, Bhopal 462037, Madhya Pradesh, India;
Email: eishaganju26@gmail.com

ISSN: 2231-2188 (Print)

ISSN: 2231-685X (Online)

Received: 17.03.2024

Revised: 20.04.2024

Accepted: 05.05.2024

Published: 10.06.2024

think these complications may be the result of inflammation triggered by your immune system. Some of these issues go away when the colitis is treated.²

Ulcerative colitis can occur in people of any age, but it usually starts between the ages of 15 and 30, and less frequently between 50 and 70 years of age. It affects all sexes equally and appears to run in families, with reports of up to 20% of people with ulcerative colitis having a family member or relative with ulcerative colitis or Crohn's disease. In addition, about 20% of people are diagnosed before they're 20 years old, and it can occur in children as young as 2 years of age. Ulcerative colitis is a lifelong condition that can have mild to severe symptoms. For most people, the symptoms come and go. Some people have just one episode and recover. A few others develop a nonstop form that rapidly advances. In up to 30% of people, the disease spreads from their rectum to their colon. When both your rectum and colon are affected, ulcerative symptoms can be worse and happen more often.³

Ulcerative Colitis (UC) is a chronic inflammatory bowel disease (IBD) characterized by inflammation of the colon and rectum. It is a relapsing and remitting condition, meaning that patients experience periods of active disease followed by periods of remission. The exact etiology of UC is not fully understood, but it is believed to involve a complex interplay of genetic, environmental, and immunological factors.

The hallmark of UC is the presence of continuous inflammation in the innermost lining of the colon and rectum, leading to the development of ulcers and other characteristic symptoms. These symptoms can include abdominal pain, diarrhea, rectal bleeding, weight loss, and fatigue. The severity of UC varies among individuals, ranging from mild to severe. The impact of UC on the quality of life for affected individuals can be substantial, with symptoms often causing discomfort and affecting daily activities. Complications such as colon perforation, toxic megacolon, and an increased risk of colorectal cancer can also arise in severe cases. Diagnosis of UC typically involves a combination of clinical evaluation, endoscopic procedures (such as colonoscopy), imaging studies, and laboratory tests. Once diagnosed, treatment strategies aim to induce and maintain remission, alleviate symptoms, and prevent complications. Medications, including anti-inflammatory drugs, immunosuppressants, and biologics, are commonly used in the management of UC.⁴

The overall prevalence rate for inflammatory bowel disease (IBD) has been reported to be 6.8 million and among them the prevalence rate of ulcerative colitis (UC) is high. The high rates are reported in the industrial areas. There are several treatments till now attempted to treat UC, however, they succeeded up to some extent only. So, the need of therapy for treatment of UC has become very important nowadays. UC's treatment options can be categorized into two attempts,

first, that alters the presumed pathogenesis of UC and second, that controls the severity and symptoms of UC. Many patients experience the relapse of UC and proliferation of disease during their clinical course. Its therapy has been divided as maintenance therapy, induction therapy, treatment for refractory disease followed by surgery. Out of these, efficacious acute therapy and safe maintenance therapy play important role in treatment of UC. There are three main classes of agents that have been used for treatment of UC. These include corticosteroids, immunomodulators and mesalamine (MES). MES is also popularly known as 5-aminosalicylic acid (5-ASA). Antidiarrheal and antispasmodic preparations have also been reported to control the severity and symptoms of UC. Other preparations like antipsychotic, antidepressants and sedatives are not recommended as a daily dose but their low doses are recommended to ameliorate symptoms in UC patients.⁵

Till date, MES is first line drug for UC. Various colon targeted drug delivery systems are previously reported for MES. These include, guar gum and Eudragit S100 coated mini tablets, hydroxy propyl methyl cellulose E 15 and Eudragit S100 based press-coated tablets, chitosan/Eudragit S100 based mesalamine microspheres, guar gum/xanthan gum based microspheres. However, these formulations were reported to have certain limitations such as premature drug release during diseases state in case of pH dependent delivery system as the pH of GIT changes and incomplete drug release in case of polysaccharide-based delivery systems due to loss of gut microflora. In recent years, several attempts have been made to develop oral formulation of MES along with other drugs/probiotics/prebiotics to get successful treatment. This approach has been taken into account because imbalance of the colonic micro flora is one of the major causes for the disease.⁶

In recent years, silver nanoparticles (AgNPs) and modified apple polysaccharide (MAP) have been explored for treating UC due to their anti-inflammatory properties. During UC, inflammation occurs due to the release of prostaglandin and chemotactic substances like interleukin-1 (IL-1), complement factors, TNF- α and tumor growth factor- β (TGF- β). AgNPs are able to suppress the activity of these inflammatory markers. In colorectal cancer cells, MAP induces apoptosis via caspase-dependent mechanism. MAP is also known to inhibit lipopolysaccharide (LPS) induced toll-like receptor 4 (TLR4) as well as Nuclear Factor (NF)- κ B pathway, thereby inhibiting metastatic activities.⁷

Mesalamine is a bowel-specific aminosalicylate drug that is used in the treatment of ulcerative colitis (UC) disease which is recurrent idiopathic inflammatory disorder that causes bloody stools and abdominal pain. There are a number of oral mesalamines that are commercially available, including azo-bond pro-drugs such as sulfasalazine, olsalazine, and

balsalazide. Delayed and controlled release dosage forms of mesalamine still appear to be insufficiently selective. This is due to the fact that drug release mechanism is based on physiological parameters that are not related to the inflammation and barely to its location. Controlled release preparations are designed to achieve optimum delivery of the biologically active mesalamine to the colon and to minimize the systemic absorption. In the case of ulcerative colitis disease, poor adherence of mesalamine has shown to be an important barrier in successful therapy and therefore, carrier systems such as nanoparticles can exclusively deliver the drug to the inflamed regions after oral administration for a prolonged period. These systems have several advantages over the conventional chemical inflammatory compounds including minor side effects.⁸

In the recent years several studies have been reported on the application of natural polymers for colon delivery. Chitosan is the N-deacetylated product of chitin, which is the second most abundant polysaccharide in nature. It has attracted great attention in the field of colon delivery. The difference between chitin and chitosan is the functional group which is situated at C₂ of the monomeric unit. Due to the presence of the amino group in chitosan it can be indicated that chitosan, has higher solubility in comparison with chitin. In addition chitosan has received great attention in the medical, biological, and pharmaceutical area due to its unique characteristics including biodegradability and biocompatibility. It has been demonstrated that this natural polymer is non-toxic which makes it an excellent candidate for drug delivery systems. Microspheres, microgels, and nanoparticles are various forms of chitosan-based drug delivery systems that have been studied extensively in the recent years.

Chitosan nanoparticles have the potential to be used as hydrophilic carrier systems since they can deliver drugs to specific sites and control the drug release rate. Different techniques can be employed to produce chitosan nanoparticles including ionic gelation, coacervation, emulsion coacervation, and reverse micellar. The most common method for this purpose is the ionic gelation which has several advantages over other methods. This method has mild conditions without applying harmful organic solvents and heat that can damage sensitive proteins. This process can be simply performed by sodium tripolyphosphate (TPP) as a cross-linking agent. The mechanism of nanoparticle formation is based on electrostatic interaction between the positively charged amino group of chitosan and the negatively charged group of TPP. TPP is a favorable cross-linker for the ionic gelation process due to its non-toxicity and quick gelling ability. The prepared nanoparticles possess a positive surface charge which makes them quit suitable for mucosal adhesion applications.⁹

MATERIALS AND METHODS

Materials

Sodium citrate and MES were procured from Hi Media Pvt. Ltd. Ethanol, sulphuric acid, copper acetate, aerosil (A-200), hydroxy furfural acetate, disodium hydrogen phosphate, potassium dihydrogen phosphate and trehalose were purchased from central drug house (CDH) Pvt. Ltd., New Delhi, India. Micro crystalline cellulose, lactose, hydrochloric acid, potassium chloride and acetic acid were purchased from Lobacheime, Mumbai, India.

Development of calibration curve for silver nitrate (AgNO₃)

AgNO₃ (100 mg) was weighed and transferred into 10 mL of standard volumetric flask and dissolved in 10 mL of water to obtain a concentration of 10 mg/mL of stock solution. Then 1.94 g of solution of potassium chromate (K₂CrO₄) was prepared in 10 mL of water and 2–3 drops of this solution was added into stock solution. Aliquots of standard solution ranging from 5 to 25 µg/mL were transferred into series of 10 mL of volumetric flasks. The absorbance of prepared dilutions was measured at 285 nm.¹⁰

Preparation of MAP solution

Apples (500 g) were cut and crushed in a mortar pestle. Crushed apples were taken in a 500 mL glass beaker and soaked overnight in ethanol to remove fatty materials. This dispersion was boiled 3 times for 8 h each time with absolute ethanol for 24 h to extract the components dissolved in ethanol. Ethanol was removed and solid mass was dried in an oven at 60 °C for 8 h. The residue was boiled in water at 100 °C three times for 8 h for extraction of polysaccharides. The aqueous extracts were combined and mixed with concentrated ethanol solution (75 mL/ L) to precipitate the fraction that were rich in polysaccharide. This was followed by removal of proteins by freeze-thawing method. The MAP was obtained through dialysis. Dialysis was carried out by keeping the apple solution (5 mL) inside the dialysis bag having molecular-weight cut off (MWCO) limits of 2000 Da. The membrane fixed with a dialysis tubing closure in the dialysis chamber filled with 200 mL of phosphate buffer saline (dialysate) was kept on a magnetic stirrer and stirred at 50 rpm. The study was carried out at room temperature for 2 h and then the dialysate was replaced with fresh one. The dialysis was carried out for another 2 h and once again the old dialysate was replaced with fresh one. Then the study was continued till 72 h. The dialyzed sample was concentrated. The concentrated samples were lyophilized using Freeze dryer (EBT-12 N, Chennai, India). The obtained residue of MAP (10 mg) was hydrolyzed with 1 mL of 2 N trifluoroacetic acid at 105°C for 8 h. Dried sample was neutralized using 3 N sodium hydroxide maintained at pH

7.0. The yield (%) of MAP was calculated as the ratio of the quantity of liquid MAP obtained after the entire extraction procedure divided by the initial amounts of raw apples taken for extraction and the ratio was multiplied by hundred. Ten different aqueous solutions of MAP with strengths ranging from 0.5 to 5% v/v with an increment of 0.5, were prepared and kept undisturbed for 30 min.¹¹

Preparation of AgNPs

For the preparation of AgNPs, 5 mM solution of AgNO₃ was added to 10 mL aqueous solution of MAP of varying concentrations (0.5%v/v-5% v/v). The prepared solutions were stoppered and kept in dark for 1 h. After this, slight change in color from colourless to light brown was observed in all the concentrations. All the solutions were scanned using UV-Visible spectrophotometer to confirm the synthesis of AgNPs. For the evaluation of stability and selection of final formulation, the UV scan of the prepared solutions was taken in the wavelength range of 400–800 nm for 3 consecutive days.¹²

Loading of MES in AgNPs

Development of calibration curve of MES

MES (10 mg) was weighed and transferred into 10 mL of standard volumetric flask. The solution was further diluted into 10 mL of 0.1 N hydrochloric acid (HCl) to obtain the concentration of 100 µg/mL. For calibration curve of MES, different aliquots were taken from the above solution and solutions of different concentrations (4, 8, 12, 16 and 20 µg/mL) were prepared in 10 mL of HCl. The absorbance was recorded at the wavelength of 324 nm and the calibration curve for MES was plotted between the concentrations versus absorbance.¹³

Loading of MES to AgNPs (AgNPs-MES)

It is important to note that among all the prepared AgNPs, nanoparticles prepared using 3.5% v/v of MAP were found more stable, hence, this solution was selected for further studies. This solution (10 mL) was taken in 50 mL glass beaker and 23 mg of MES was dissolved in it.¹⁴

Characterization of synthesized AgNPs-MES

Surface plasmon resonance (SPR)

SPR for final formulation of AgNPs and AgNPs-MES was recorded in the range of 200–600 nm to confirm the formation of AgNPs and AgNPs- MES. The overlay of both the spectrum was recorded.¹⁵

Dynamic light scattering (DLS)

Size distribution, polydispersity index and zeta potential of the prepared AgNPs and AgNPs- MES were measured using Zetasizer ZS90. A laser beam of 50 mV was projected on the

plastic sample cells at an angle of 90°. Samples (1 mL) were diluted to 10 mL using distilled water and analyzed. The analysis was carried out in triplicate and their mean value was recorded.¹⁶

Transmission electron microscopy (TEM)

The shape of AgNPs and AgNPs-MES was analyzed through TEM (JEM 1010; JEOL, Tokyo, Japan). Phosphotungstic acid of 2% w/v concentration was used to stain the formulations. Afterwards they were applied on copper grid and allowed to dry in air. Images were then recorded at a scale bar of 200 nm.¹⁷

Release study in bio-relevant media

The release study was performed for MES and AgNPs-MES in medium containing rat caecal contents (RCC) as well as in medium without rat caecal content (WRCC) using paddle apparatus. Speed of paddle was kept at 50 ± 4 rpm and temperature of medium was kept at 37 ± 0.5°C. Samples (10 mL) were added to dissolution vessels. First step of the study was performed in 200 mL of 0.1 N HCl for 2 h. At the end of second hour, 700 mL of phosphate buffer (0.2 M; pH 6.8) was added to the same medium and the pH of medium was adjusted to 6.8 using sodium hydroxide solution (0.2 M). The confirmation of pH throughout the study was done using pH meter. The total volume of medium became 900 mL. It is important to note that addition of 4–5% w/v of rat caecal contents in dissolution medium is recommended to achieve sufficient number of microbes/enzymes to degrade the polysaccharide matrix/coat. The final volume of vessel was adjusted to 1000 mL. The study was continued for 24 h with constant purging of CO₂ for achievement of anaerobic conditions. After every 1 h, samples (5 mL) were withdrawn and replaced by 5 mL of blank solution to maintain sink conditions up to 24 h. The samples were evaluated by UV-Visible spectrophotometer at the wavelength of 324 nm.¹⁸

In vitro cell line toxicity study

Cytotoxicity assays was carried out by 3-(4,5 dimethyl thiazole-2-yl)-2,5-diphenyl tetrazolium bromide (MTT) assay using Caco-2-cells. Cell culture was centrifuged and the cell density of the suspension was adjusted to 1.0 × 10⁵ cells/mL. Dulbecco's Modified Eagle Medium (DMEM) containing 10% FBS was used as the culture medium. An amount of 100 µL of this diluted inoculum (approximately 10,000 cells/well) was added per well of a 96 well flat bottom micro titre plate. Serial dilution of AgNO₃, AgNPs and AgNPs-MES were prepared in the range from to 4 µg/mL to 250 µg/mL. After 24 h, the cells were centrifuged, supernatants were removed and the pellets were suspended with 100 µL of the test samples of different strengths prepared in maintenance media. These plates were kept in humidified incubator at 37 °C for 48 h with a 5% CO₂ atmosphere and examined

microscopically every 24 h. After 48 h, serial dilutions of these samples were prepared, centrifuged and the pellets were re-suspended with 20 µL of MTT (2 mg/mL) in phenol red free minimum essential medium (MEM-PR). The plates were gently shaken and incubated for 15 min at 37 °C in 5% CO₂ atmosphere. A quantity of 100 µL of DMSO was added and the plates were gently shaken to solubilize the formed formazan. Absorbance was measured at a wavelength of 540 nm using a micro plate reader. The percentage cell viability was calculated using equation (2) while the strength of the sample required to inhibit cell growth by 50% was calculated by plotting dose response curve.¹⁹

$$\% \text{ Cell viability} = \frac{\text{Mean optical density of individual test solution}}{\text{Mean optical density of standard solution}}$$

In vivo study animal study for treatment of UC

The study was carried out using 54 animals with six animals in each of the nine groups as shown in Table 1. Rats (Sprague Dawley) of either sex, weighing between 250 and 300 g, were purchased from NIPER, Mohali, India. The study was approved by Institutional Animal Ethics Committee (IAEC Protocol Number: LPU/IAEC/2019/45). The animals were kept under light and dark cycles of 12 h at 25 ± 2 °C for 10 days prior to initiation of study and fed with standard rat chow diet and water *ad libitum*.

Induction of colitis and treatment of UC

The UC was induced to rats by intracolonic administration of 0.2–0.3 mL of acetic acid (AA) using propylene tube (0.2 mm diameter). The tube was dipped in glycerine and inserted through rectum up to a length of 7–8 cm in colon. After administration of AA, animals were held in supine Trendelenburg position for 15 sec.

Treatment protocol

Rats of Group 1 were administered 1 mL of normal saline orally for 14 days. Rats of Group 2– 9 were treated with AA as mentioned in 2.10.1 for induction of UC. Group 2 rats did not receive any treatment for next 14 days after induction of UC, whereas, after induction of UC (i.e. 72 h) the rats of other groups were given the respective treatment as mentioned in Table 1 for 14 days.²⁰

Estimation of UC

Disease activity index (DAI)

Stool consistency

The consistency of stools of each animal of each group was observed on the 0th, 7th and 14th day of study. The DAI was determined by referring the scale of stool consistency as per standard protocol.

Weight loss

Weight loss for each animal of each group was observed on 0th, 7th and 14th day of the study, DAI was determined by adding the scale of the weight loss as presented.

Biochemical estimation

Estimation of reduction in glutathione (GSH) levels

GSH was estimated by homogenizing colonic tissue (720 µL) with 5% w/v trichloroacetic acid (TCA). The homogenate was centrifuged at 10,000 g for 5 min to precipitate tissue matrix. The supernatant was mixed with Ellman's reagent/5,5' dithio bis (2 nitrobenzoic acid) and their absorbance was recorded at 412 nm. A calibration curve was plotted using different strengths of standard GSH solution. The concentration of GSH present (nmol/mg protein) in tissue homogenate was calculated using the regression equation obtained from calibration curve.²¹

Estimation of thiobarbituric acid reactive substances (TBARS)

TBARS is used as a marker for lipid peroxidation. Its levels in the samples were calculated by estimating the strength of MDA. To calculate this, three different solutions *viz* 0.1 M Tris-HCl buffer (pH 7.4), thiobarbituric acid (TBA, 0.67% w/v) and 10% w/v TCA were prepared. Colonic tissue homogenate (1 mL) was mixed with 1 mL of Tris-HCl in a test tube centrifuged at 1000 g for 10 min and supernatant (1 mL) was mixed with TBA solution. The mixture was heated at 50°C for 2 min and cooled. To the cooled solution, distilled water (1 mL) was added and absorbance was determined at 532 nm. The concentration of TBARS was calculated in mMoles MDA/mg protein using:

$$3 \times \text{optical density of sample} \div 0.156 \times \text{mg protein} / 0.2 = \text{nmoles of MDA/ mg protein}$$

Estimation of myeloperoxidase (MPO)

The process of homogenization was performed in 10 mL of 50 mM potassium phosphate buffer cooled in ice, having pH 6.0 and containing 0.5% w/v hexadecyl trimethyl ammonium bromide (HETAB). The prepared homogenates were sonicated for 10 min using ultra sonicator (Loba life, Mumbai, India). The sonication was followed by the process of centrifugation on a cooling centrifuge (M 1214, Remi, Vasai, Mumbai, India) at 12000 g for 20 min at 4°C. A sample of 0.1 mL from the supernatant was withdrawn from each tube and mixed with 2.9 mL of phosphate buffer (pH 6.0) containing 0.0005% v/v H₂O₂. UV spectrophotometer was used to measure the change in absorbance per minute (Shimadzu UV 1800, Japan) at 460 nm. A single unit of MPO is defined as the change in absorbance per minute by 1.0 unit at room temperature. It was calculated by:

$$\text{MPO activity (U/g)} = X \chi \text{ Weight of tissue taken}$$

where, $X = 10 \times$ change in absorbance/minute/volume of supernatant taken in final reaction

Estimation of superoxide dismutase (SOD)

Isolated colonic tissue was homogenized in a mixture of sodium pyrophosphate buffer (1.2 mL), 0.1 mL of phenyl methane sulphonyl fluoride (PMSF), nitro blue tetrazolium (0.3 mL) and enzyme preparation (0.2 mL). The total volume was adjusted to 2.8 mL using water. For initiating the reaction, Nicotinamide Adenine Dinucleotide Hydrogen (2 mL) was added to the mixture and incubated for 90 s. The reaction was stopped by addition of 1 mL of glacial acetic acid. To this, n-butanol (4 mL) was added and kept aside for 10 min. This mixture was centrifuged at 5000 g for 10 min and the intensity of the chromogen present in the butanol layer was measured at 560 nm "A single unit of enzyme activity can be defined as the net amount of enzyme required to give an inhibition of 50% of NBT reduction in a 60s".²²

Estimation of tumor necrosis factor- α (TNF- α)

On 7th and 14th day, isolated colonic tissue was added to solution containing mixture of phosphate buffer solution, PMSF and protease inhibitor and homogenized for 15 min using tissue homogenizer at 5000 rpm for 15 min. The homogenate was sonicated and sodium lauryl sulphate was added to it. Afterwards, the homogenate was kept in ice cold water for 30 min. It was sonicated again and centrifuged at 10,000 g for 10 min at 4 °C. The supernatant was separated and level of TNF- α was estimated using ELISA kits from eBiosciences (USA).²³

Histopathological examination

The colonic tissues (4 cm length) were excised on seventh and fourteenth day. These tissues were weighed and fixed in 10% v/v of neutral buffered formalin solution for 24 h. Transverse sections of these tissue were embedded in paraffin blocks. Staining of isolated tissue was done using haematoxylin-eosin (HE) and subjected to histopathological examination by qualified pathologist. Imaging was done using x 40 lens. The parameters used to assess colonic tissue's damage include crypt's loss, loss of integrity of mucosal epithelium, and extent of inflammation.²⁴

Statistical analysis

The obtained results from the experiment were expressed as mean \pm SD. The graphs were plotted using Graph Pad Prism version 7.0 (Graph Pad software INC., CA, USA). The results were compared using analysis of variance and Student 't' test. The $P < 0.05$ (wherever, applicable) value indicated significant difference in the results. The similarity factor (f_2) was calculated using model independent analysis and value between two dissolution profiles above 50 indicated similarity between.²⁵

RESULTS AND DISCUSSION

The calibration curve of AgNO_3 was recorded and it was found linear in the range of 5–25 $\mu\text{g/mL}$ as the coefficient regression (R^2) was found to be 0.992. The extracted MAP was characterized for density, molecular weight, polysaccharide content. The density of prepared MAP solution was found to be (1.03 g/mL) which was in agreement with our previously published work. The yield of MAP was 55%. Further, the major components of MAP were galactose and galacturonic acid. The molecular weight of MAP was 2500–3000 Da and the amount of sugar was more than 85% and protein content was less than 3%. These were found in concordance with previously published research works.

Preparation of AgNPs

The AgNPs prepared exhibited their absorbance maxima i.e. SPR at 400 nm. This absorption at 400 nm is due to excitation of surface plasmon vibration by colloidal silver nanoparticles. The results indicated maximum absorbance of AgNPs containing 3.5% v/v MAP indicating maximum formation of AgNPs at this concentration as compared to those formed using other concentrations of MAP. Hence, this formulation was selected for conjugating MES.

Characterization of optimized AgNPs-MES

Encapsulation efficiency

It is important to note that the absorbance maxima (SPR) of AgNPs- MES nanoparticles was found at 383 nm (Figure 1). The encapsulation efficiency of MES in AgNPs was found to be $93 \pm 3.21\%$. A decrease in intensity of absorbance maxima and blue-shift in SPR of AgNPs from 400 nm to 383 nm was observed after loading of MES which could be attributed to physical interaction and increased electrostatic repulsions between the colloidal silver nanoparticles and mesalamine particles.

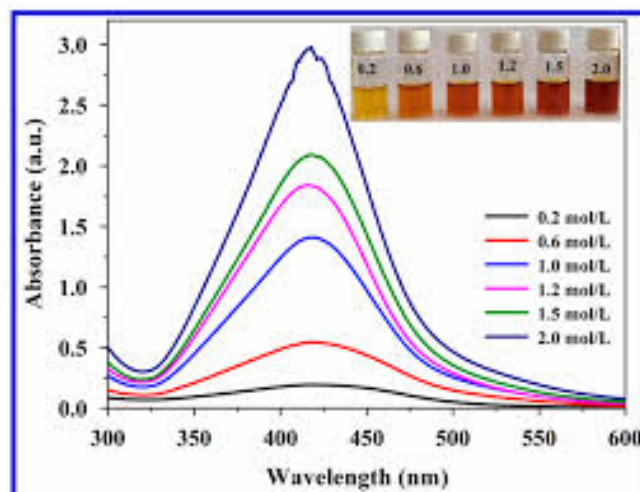


Figure 1

Particle size and zeta potential

The zeta potential for AgNPs and AgNPs-MES was found to be 16.3 ± 1.54 mV and 14.27 ± 2.16 mV. Mean particle of AgNPs and AgNPs- MES was found to be 89 ± 3 nm and 101 ± 9 nm, respectively. The polydispersity index was found to be 0.577 ± 0.08 and 0.352 ± 0.065 for AgNPs and AgNPs loaded MES, respectively. The p-value was found above 0.05 for zeta potential, particle size and polydispersity index of AgNPs and AgNPs-MES indicated absence in any significant change in these properties after loading of MES to the AgNPs. The results indicated negative charge on zeta potential of AgNPs-MES because of capping of AgNPs by MAP. MAP being a polysaccharide, possesses negative charge on it. A reduction in negative charge of zeta potential was observed upon loading of MES with AgNPs (AgNPs-MES). The complete scheme of formation of AgNPs-MES is shown in **Figure 2**. The figure illustrates the adsorption of MAP onto the surface of AgNPs and embedment of MES in the matrix of MAP- capped AgNPs. The slight increase in size of AgNPs was observed upon loading of MES.

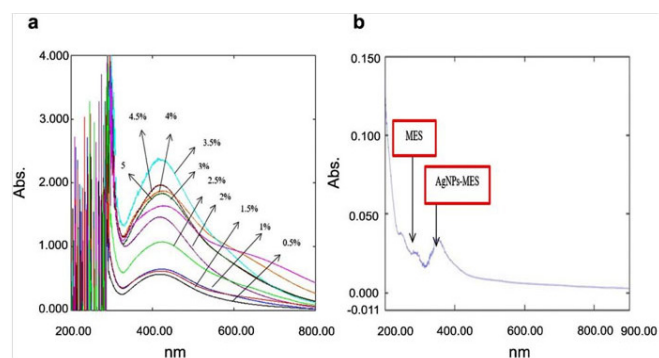


Figure 2: SPR of a. AgNPs prepared using various concentrations of MAP; b. AgNPs-MES.

The TEM images of MAP-capped AgNPs and AgNPs-MES are shown in **Figure 3**. The images revealed formation of spherical nanoparticles. The average size obtained from TEM analysis for AgNPs was 91.75 ± 3.21 nm and AgNPs-MES was 103.59 ± 4.02 nm, whereas, the size obtained from DLS studies was 89 ± 3 nm for AgNPs and 101 ± 9 nm for AgNPs- MES. Hence, a non-significant difference ($p > 0.05$) in results of particle size indicated a better correlation between the results of particle size obtained from DLS and TEM studies. The images also showed increase in size upon loading of AgNPs with MES (**Figure 3**).

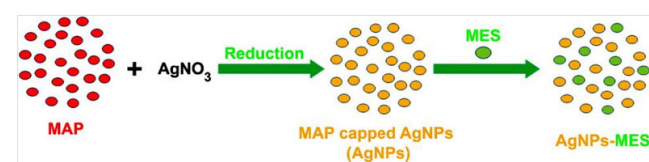


Figure 3: Schematic representation of preparation of AgNPs-MES.

In vitro drug release study

AgNPs-MES were subjected for drug release studies for 24 h in a medium containing RCC as well as WRCC. The results revealed of AgNPs-MES subjected in WRCC revealed only $46 \pm 2\%$ release of MES from the formulation in the first 5 h. This indicated slow and sustained diffusion of MES (about 50% release) from the matrix of polysaccharide (MAP) for first 5 h i.e. upper GIT. The results indicated that 54% release of MES got restricted in the upper GIT because of drug loaded nanoparticles entrapped in the matrix, of MAP, which is a polysaccharide (**Figure 4**). Even after 24 h, the maximum drug release was found to be only $60 \pm 2\%$. This was due the unavailability of microbiota that could have degraded the polysaccharide matrix. Whereas, in the case of formulation subjected to medium containing RCC, the drug release from AgNPs-MES was found $41 \pm 5.18\%$ in first 5 h (i.e. about 59% restriction of drug release in upper GIT). Upon addition of the rat caecal content (RCC) at the end of the 5th h, a sudden rise in the drug release was observed at the end of 6th h ($85 \pm 3\%$). Almost complete drug got released ($98 \pm 2\%$) within 12 h of the study and at the end of 24 h the release was found to be $100 \pm 9\%$. It is important to note that in both the cases, the drug release profiles were similar till first 5 h ($f_2 = 95$; $p = 0.70$), indicating sustained release pattern. When the formulation came in contact of RCC (i.e. after 5 h), an immediate burst release of MES was observed in case of formulation subjected in medium containing RCC as compared to the one in which RCC was not added ($f_2 = 19$; $p < 0.0001$).

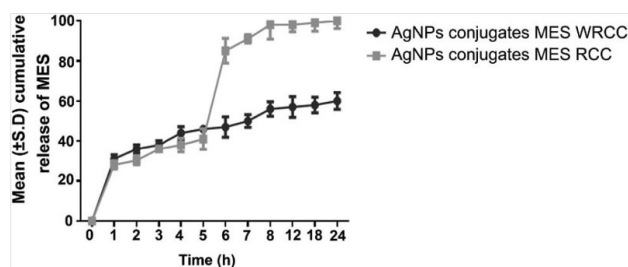


Figure 4: In-vitro drug release study of AgNPs-MES in RCC and WRCC.

In vitro cell line toxicity study

More than 86% of the cells were found to be viable at concentration of $4 \mu\text{g/mL}$ for AgNPs- MES while 77% of the cells were viable in case of treatment with AgNPs alone (**Figure 5**). Metallic nanoparticles are known to cause cellular toxicity but in the present study cellular protection for more than 50% cells in case of AgNPs could be due to presence of MAP which is known to possess anti-ulcer and antioxidant activity [11]. Further enhanced cellular protection was observed in case AgNPs-MES as that of AgNPs alone due to anti-ulcer and anti- inflammatory action

of MES. It is important to note that the dose of AgNPs used in the present study was 4 mg/kg body weight of rats. This means 1 mg dose for 250 g of rats has been administrated. This indicated 4 µg/g (equivalent to 4 µg/mL) of AgNPs have been administrated which are found to be safe in cell line studies.

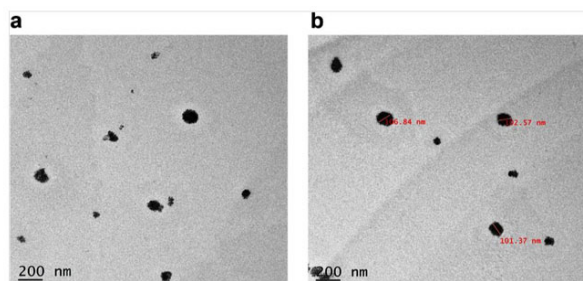


Figure 5: Results of cell viability for AgNO₃, AgNPs and AgNPs-MES at different concentrations.

Antioxidant and inflammatory markers

The efficacy of AgNPs-MES was evaluated through different pharmacodynamics studies conducted on acetic acid induced UC in rats. Various parameters like MPO, SOD, GSH, TBARSs and TNF-α were estimated. MPO is an enzyme which found in the neutrophil and used as an indicator for neutrophil infiltration of the tissues. This activity is also used as a marker for the inflammatory process in the intestine. The results of MPO obtained from samples collected on 7th and 14th day (**Figure 6**) indicated significantly higher MPO values ($p < 0.05$) in group 2 as compared to all the other groups. This was due to the fact that the rats of group 2 received no treatment after induction of UC and rest of the UC induced groups (groups 3 to 9) who received treatment, showed recovery of different extent based upon the efficacy of their treatment. The maximum recovery (i.e. decrease in MPO level) was observed in rats of group 9 who received high dose of AgNPs-MES, followed by group 8 who received low dose of AgNPs-MES. The treatment efficacy of group 8 and 9 was found better as compared to rats of group 5 and 6. This clearly indicated increase in treatment efficiency of AgNPs upon their co-administration with MES (group 8 and 9). Furthermore, it is important to note that the dose of MES was same for rats of group 8 and 9, hence, the improved results with rats of group 9 as that of group 8 and group 6 as that of group 5 was due to increase in dose of AgNPs. This clearly indicated potential of AgNPs as anti-ulcer agent. The results also indicated that there was no significant difference in the MPO activity of group 8 and 9 as compared to the group 1 (normal control $p > 0.05$). This was followed by rats of group 7 who received treatment of combination of MAP and MES as compared to rats of group 3 to group 6. MES is first line drug to treat UC and MAP has also been reported for its anti-ulcer potential (REF). Hence, co-administration

of these two have shown better anti-ulcer potential as that of MAP alone (group 3), MES alone (group 4) and AgNPs at both doses (groups 5 and 6). The decreasing order of MPO level on 7th and 14th days was in the following order:

group 2 > group 3 > group 4 > group 5 > group 6 > group 7 > group 8 > group 9 > group 1

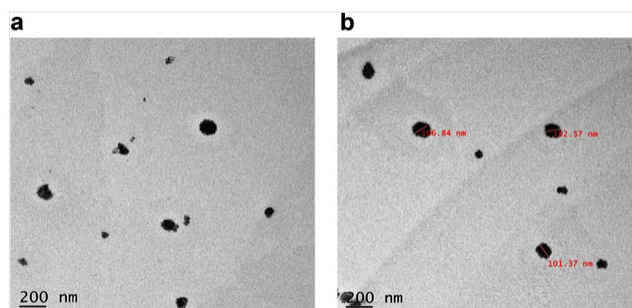


Figure 6: TEM images of A. MAP-capped AgNPs (AgNPs) and B. AgNPs-MES.

The levels for TBARs and TNF-α for various treatment groups were found same as that of MPO whereas, the levels of GSH and SOD were found opposite to that of MPO. The decreasing order of GSH and SOD was found in the following order:

group 1 > group 9 > group 8 > group 7 > group 6 > group 5 > group 4 > group 3 > group 2

The result of these parameters also indicated that the combination treatment of MAP, MES and AgNPs was able to reduce the inflammation of the intestine successfully.

Estimation of treatment on the colonic weight ratio in acetic acid induced UC rat model

The colonic weight ratio was determined for isolated colon of all the groups (group1 to group 8) that were sacrificed on 7th and 14th day respectively. There was a significant increase ($P < 0.001$) in the colonic weight ratio for the rats from the group 2 to group 7 as compared to the group 1. However, the weight ratios of the colons of the rats of group 8 and 9 were found closer to the group 1. It was very important to notice that more colonic weight ratio signifies more inflammation to colonic and more damage. The colonic weight ratios of the different groups were found in the following increasing order on 7th as well as 14th days (**Figure 7**).

group 1 < group 9 < group 8 < group 7 < group 6 < group 5 < group 4 < group 3 < group 2

Estimation of disease activity index (DAI)

DAI score was determined on 0th, 7th, and 14th day of the study in the treatment groups. To evaluate DAI, each of the individual scores of the parameters like percentage loss

of weight and consistency of stool were determined. The overall DAI for individual rat was determined by addition of individual scores followed by dividing the total score by two. The interpretations of overall DAI for different groups are shown in Fig. 7b–d. The day of administering acetic acid through the rectal route is considered as day 0 and hence no sign of UC was observed. On the 7th day after the induction of UC, experimental control group (group 2) animals suffered the maximum % weight loss. Thus, this group showed a significant rise in the DAI score as compared to normal control (group 1) with $p < 0.001$. But a significant difference was seen in the DAI score when group 2 was compared with group 8 and group 9 ($p < 0.001$) and group 3 and group 4 ($p < 0.05$). On the 14th day of the study, the stool consistency in groups 8 and 9 were normal. The DAI score revealed that group 8 and group 9 did not have any significant difference with group 1 (normal control) with $p > 0.001$ whereas, group 3 and group 4 showed a significant difference as compared to

group 2 ($p < 0.001$). The rats of groups 5 and 6 who received only AgNPs treatment have also shown better recovery, however, it was significantly less ($p < 0.05$) as that of groups 8 and 9, indicating the potential of co-administration of MES with AgNPs. The value of DAI score is directly proportional with the severity of the disease. The score was maximum in case of group 2 and minimum in group 1 after two days of the induction of the disease. A treatment regime of 14 days was provided to the UC induced rats. All the groups showed a certain level of reduction in the DAI score after the complete treatment regime and followed the following pattern of reduction:

group 9 > group 8 > group 7 > group 6 > group 5 > group 4 > group 3

which confirmed the efficacy of the combined dose of MAP, MES and AgNPs over their single treatment regime.

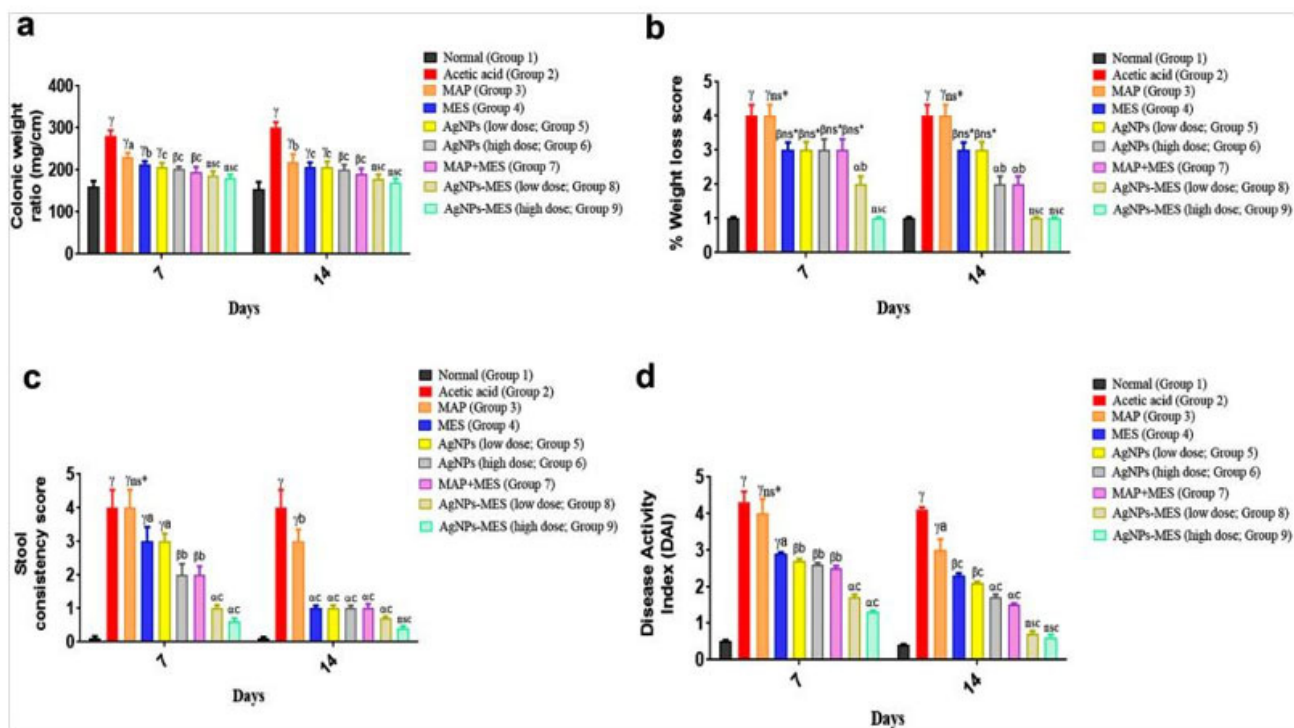


Figure 7: Results of a. colonic weight; b. %weight loss; c. stool consistency; d. overall DAI. Data analysis was done by one-way analysis of variance, followed by Bonferroni's multiple comparison test. Results are expressed as mean \pm SEM ($n = 6$), $\alpha = P < 0.05$, $\beta = P < 0.01$, $\gamma = P < 0.001$, ns = not significant as compared to the normal control group; a = $P < 0.005$, b < $P.01$, c = $P < 0.001$ compared to the experiment control group; ns* = not significant as compared to the experimental control group.

Histopathological examination

Microscopic examination of all the isolated tissue was carried out and the details of histopathological impressions are shown in **Table 1** and images are shown in **Figure 8**. The

result of the histopathological study supports the results of DAI and other parameters of UC treatment obtained in the entire study.

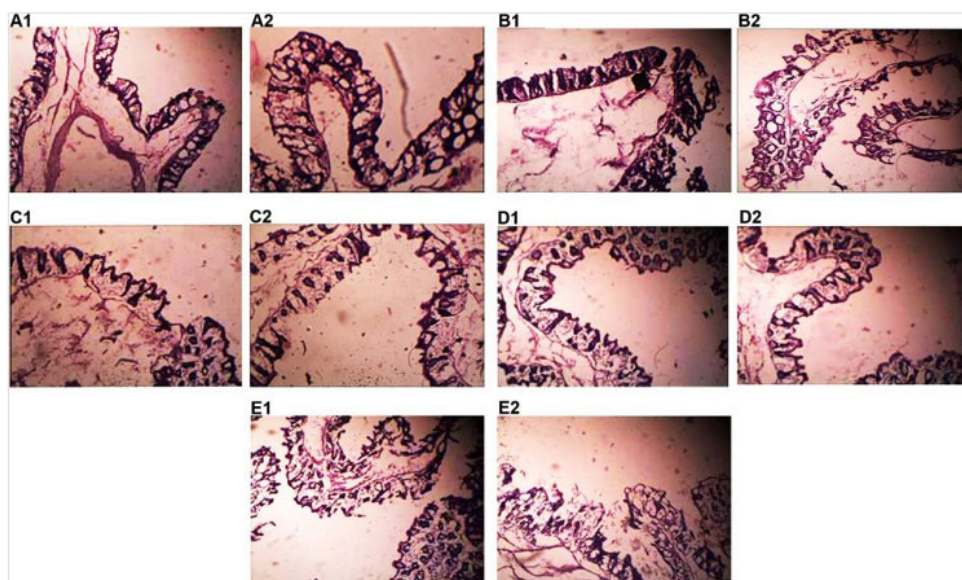


Figure 8: Histopathological images of colonic tissues of rats of group 1 (A), group 2 (B), group 3 (C), group 4 (D) and group 5 (E). Note: Numeric 1 shows histopathology of rats' colon on day.

Table 1: Histopathology report of transverse section of colonic tissue.

Group 1	Normal Control (NG)	7th (A1)	Normal looking mucosa with no lesions of pathological significance
		14th (A2)	Normal looking mucosa with no lesions of pathological significance
Group 2	Experimental control (EC)	7th (B1)	Diffused active colitis; superficial erosions, stromal edema, dense acute and chronic inflammatory cells infiltrate with widely ulcerating mucosa
		14th (B2)	Diffused active colitis; superficial erosions, stromal edema, dense acute and chronic inflammatory cells infiltrate with widely ulcerating mucosa but with less severity
Group 3	MAP solution	7th (C1)	Fewer rise in number of goblet cells, slight disruption of epithelial lining; low neutrophilic infiltration
		14th (C2)	Very slight disruption of epithelial lining; negligible neutrophilic infiltration.
Group 4	Mesalamine	7th (D1)	Damage of crypt cells; rise in number of goblet cells, disruption of epithelial lining; neutrophilic infiltration
		14th (D2)	Slight damage in the crypt cells; negligible surface epithelial loss, neutrophilic infiltration
Group 5	AgNPs (Low Dose)	7th (E1)	Moderate neutrophilic infiltration; negligible disruption of epithelial lining.
		14th (E2)	Low neutrophilic infiltration; negligible disruption of epithelial lining.
Group 6	AgNPs (High Dose)	7th (F1)	Low neutrophilic infiltration; negligible disruption of epithelial lining.
		14th (F2)	Negligible neutrophilic infiltration; negligible disruption of epithelial lining.

CONCLUSION

The research presented in this thesis focused on the development and characterization of mesalamine-loaded nanoparticles as a novel and effective drug delivery system for the treatment of ulcerative colitis (UC). UC is a debilitating chronic inflammatory condition of the colon, where existing therapeutic options are often limited by inadequate drug targeting, suboptimal bioavailability, and adverse systemic effects. This study aimed to overcome these challenges by utilizing nanotechnology to enhance the therapeutic potential of mesalamine, a widely used first-line treatment for UC. Mesalamine nanoparticles were successfully formulated using a solvent evaporation technique, optimizing critical parameters such as particle size, morphology, and drug loading efficiency. Comprehensive characterization confirmed that the nanoparticles exhibited a small and uniform size distribution (mean size of 150 ± 20 nm), high encapsulation efficiency ($85 \pm 5\%$), and a stable structure, making them suitable for targeted drug delivery applications. The sustained release of mesalamine from the nanoparticles, demonstrated through in vitro drug release studies, offers a significant improvement over conventional formulations, ensuring prolonged therapeutic efficacy and reducing dosing frequency. In vitro biocompatibility and anti-inflammatory assays further validated the nanoparticles' safety and efficacy, showing that they significantly reduced pro-inflammatory cytokine levels in human intestinal epithelial cells (Caco-2). The nanoparticles' ability to deliver mesalamine directly to the site of inflammation in the colon was confirmed through in vivo studies using a dextran sulfate sodium (DSS)-induced UC model in rats. The mesalamine nanoparticles exhibited enhanced therapeutic outcomes compared to free mesalamine, as evidenced by improved colon histopathology, reduction in inflammation, and overall amelioration of UC symptoms. This targeted delivery not only minimizes systemic exposure but also enhances the local therapeutic effect, a critical requirement for treating inflammatory bowel disease. Pharmacokinetic studies showed that the nanoparticulate system improved mesalamine's bioavailability, enhancing drug retention in the colon and reducing the risk of systemic side effects. Stability studies conducted under varying environmental conditions demonstrated that the mesalamine nanoparticles remained stable over extended periods, supporting their potential for real-world application and commercialization. Overall, the findings of this research clearly demonstrate the superiority of mesalamine nanoparticles over traditional mesalamine formulations. The targeted delivery system not only addresses the key limitations of conventional therapy but also opens new pathways for developing advanced treatments for UC and other gastrointestinal disorders. This study lays the groundwork for further clinical translation, including large-scale manufacturing, clinical trials, and eventual

commercialization, with the potential to significantly improve the quality of life for UC patients. The implications of this work extend beyond ulcerative colitis, suggesting broader applications of nanotechnology in drug delivery for other chronic inflammatory diseases. The sustained and localized drug delivery approach described here could be adapted for other therapeutic agents, highlighting the versatility and impact of nanoparticulate drug delivery systems. Moving forward, additional research focusing on long-term safety, large-scale production, and clinical efficacy in human patients will be necessary to bring this promising technology closer to clinical use. Nevertheless, this thesis represents a critical step toward revolutionizing the treatment of ulcerative colitis and optimizing therapeutic outcomes for patients.

ACKNOWLEDGEMENT

The authors acknowledge the help and support received from college management.

CONFLICT OF INTEREST

No Conflict of interest declared.

SOURCE OF FUNDING

No agency provided any funding.

AUTHORS' CONTRIBUTION

Bhaskar Kumar Gupta: Analysis, Plagiarism correction, Revision

Eisha Ganju: Concept, Checking, Editing, Grammar correction

Rameshwar Rajput: Literature Review, Formatting, Writing manuscript

REFERENCES

- Loftus EV. Clinical epidemiology of inflammatory bowel disease: Incidence, prevalence, and environmental influences. *Gastroenterology*. 2004;126(6):1504-17.
- Baumgart DC, Sandborn WJ. Inflammatory bowel disease: clinical aspects and established and evolving therapies. *Lancet*. 2007;369(9573):1641-57.
- Yeomans ND. Mesalamine in the treatment and maintenance of remission of ulcerative colitis: a review of clinical experience. *Therapeutic Advances in Gastroenterology*. 2011;4(4):237-48.
- Nunes R, Silva C, Barbosa J, Freitas J, Almeida AJ, Silva R. Nanotechnology-based delivery systems for the treatment

- of inflammatory bowel disease: from bench to bedside. *Acta Biomater.* 2020;114:210-31.
5. Sinha VR, Kumria R. Microbially triggered drug delivery to the colon. *Eur J Pharm Sci.* 2003;18(1):3-18.
 6. Abed SN, Al Matar MA, Al-Ghazali HH, Abd Aljabbar SA. Development and characterization of mesalamine loaded nanoparticles for ulcerative colitis therapy. *J Drug Deliv Sci Technol.* 2021;61:102184.
 7. Yao J, Zhou JP, Ping QN, Lu Y, Chen L, Zheng CZ. Mesalamine loaded solid lipid nanoparticles for targeted therapy of ulcerative colitis: Characterization and biodistribution. *Colloids Surf B Biointerfaces.* 2015;125:10-7.
 8. Gaspar MM, Calado S, Pereira J, Ferronha H, Correia IJ, Castro GA. Nanoparticles for targeting mesalamine to inflammation sites of the gastrointestinal tract. *Int J Pharm.* 2014;468(1-2):199-206.
 9. Gionchetti P, Calabrese C, Rizzello F. Mesalamine in the prevention and treatment of pouchitis. *Best Pract Res Clin Gastroenterol.* 2012;26(1):85-90.
 10. Huang X, Shah K, Bradbury JA, Knittel J, Ge H, Carnahan MA, et al. Mesalamine nanoparticles alleviate experimental colitis in mice. *J Control Release.* 2020;322:509-23.
 11. Zhang W, Xia Q, Wu J, Xu Y, Chen W, Xu L. Nanostructured lipid carriers for the oral delivery of mesalamine to the colon: preparation, characterization, and in vivo evaluation. *Colloids Surf B Biointerfaces.* 2013;104:135-42.
 12. Patel M, Shah N, Shah R. Formulation and evaluation of mesalamine-loaded mucoadhesive microspheres for colon targeting. *Saudi Pharm J.* 2016;24(2):160-71.
 13. Prabhakar B, Shirwaikar A, Shirwaikar A, Kumar A, Jacob A. Formulation and evaluation of sustained release microspheres of mesalamine. *Indian J Pharm Sci.* 2008;70(5):557-61.
 14. Chourasia MK, Jain SK. Pharmaceutical approaches to colon targeted drug delivery systems. *J Pharm Pharm Sci.* 2003;6(1):33-66.
 15. Lamprecht A, Yamamoto H, Takeuchi H, Kawashima Y. A pH-sensitive microsphere system for the colon delivery of tacrolimus: in vitro and in vivo evaluation in rats. *J Control Release.* 2004;97(1):93-102.
 16. Mahmood S, Imran M, Saleem U, Ali JS. Development and evaluation of mesalamine-laden PLGA nanoparticles for ulcerative colitis. *Pharm Dev Technol.* 2019;24(8):939-46.
 17. Aznar E, Martínez-Mañez R, Sancenón F, Benito A, Soto J, Barat JM, et al. Controlled release of cargo molecules in the presence of inflammatory biomarkers using capped mesoporous silica nanoparticles. *Angew Chem Int Ed Engl.* 2009;48(52):9327-31.
 18. Allam A, Fetih G, Shapiro S, Fetih S, Patra HK. Mesalamine-loaded chitosan nanoparticles for enhanced anti-inflammatory activity in ulcerative colitis therapy. *Curr Drug Deliv.* 2020;17(4):311-9.
 19. Harris JG, Card DJ, Gordon S, Reyes-Romero M, Zaman M, Garza CA. Topical mesalamine therapy for ulcerative colitis: Review of a first-line treatment. *J Gastroenterol Hepatol.* 2021;36(1):126-35.
 20. Desai N, Sharma PK, Sharma P, Sharma A. Formulation and in vitro evaluation of mesalamine floating microballoons for sustained drug delivery to the upper gastrointestinal tract. *Drug Deliv Transl Res.* 2019;9(4):898-911.
 21. Choudhary S, Bansal M, Bansal A. Development and characterization of mesalamine-loaded nanocapsules for targeted delivery in ulcerative colitis. *J Drug Deliv Sci Technol.* 2021;64:102530.
 22. Yang Y, Chen X, Liu J, Zuo Z. Mesalamine microparticles coated with eudragit S100 for targeted drug delivery to the colon: preparation, in vitro and in vivo evaluation. *Colloids Surf B Biointerfaces.* 2020;195:111249.
 23. Lee SH, Bajracharya R, Min JY, Han J. Mesalamine-conjugated nanoparticles for inflammatory bowel disease treatment: preclinical study. *Int J Pharm.* 2021;593:120151.
 24. Ogata H, Matsui T, Nakamura M, Iida M, Motoya S, Watanabe M. A randomized, controlled trial of the oral treatment with mesalamine for active ulcerative colitis. *Am J Gastroenterol.* 2006;101(12):2825-32.
 25. Koch A, Gurbuz M, Hetjens S, Zosel F, Kloss F, Friedl H, et al. Development and in vivo evaluation of mesalamine nanoparticles. *Eur J Pharm Biopharm.* 2020;151:49-59.